Article

Cavity-Assisted Spin-Orbit Coupling of Ultracold atoms

Lin Dong [1], Chuanzhou Zhu [1] and Han Pu [1]*

[1] Department of Physics and Astronomy, Rice Quantum Institute, Rice University, Houston, Texas, 77251-1892, USA

* Author to whom correspondence should be addressed; hpu@rice.edu

---

Abstract: We investigate dynamical and static properties of ultracold atoms confined in an optical cavity, where two photon Raman process induces effective coupling between atom's internal degrees of freedom and center-of-mass motion. In the meantime, atomic dynamics exerts a back action to cavity photons. We adopt both mean field and master equation approach to tackle the problem and found surprising modifications to atomic dispersions and dynamical instabilities, arising from the intrinsic nonlinearity of the system. Correspondence between semi-classical and quantum limits is analyzed as well.

Keywords: cavity quantum electrodynamics; cold atoms; spin-orbit coupling

---

1. Introduction

When Jaynes and Cummings first studied the time evolution of a two-level atom in an electromagnetic field in a *fully* quantized way in 1960s [1], experimental realization of this ideal theoretical model was out of reach. It was made possible only with the advent of one-atom masers in late 1980s, by Rempe, Walther and Klein [2], to experimentally study the interaction of a single atom and a single resonant mode of electromagnetic field in a cavity. Jaynes-Cummings model (J-C Model) serves to understand the relationship between quantum theory of radiation and semi-classical theory of atom-light interaction. The field of cavity quantum electrodynamics (CQED) was further advanced by putting cold atoms into the high finesse optical cavities [3–5]. Unlike "hot" atoms, cold atoms' center-of-mass motion (COM) can no longer be neglected in this "atom + cavity" system. One needs to seek a self-consistent solution for both light and atom by treating them on equal footing. Because intra-cavity photon and

20 atoms very frequently scatter off each other due to the geometric confinement, not only dipole force
21 gets strongly enhanced but also atom's back-action *onto* light becomes significant. For Bose-Einstein
22 condensate (BEC), atoms occupy the same motional quantum state, and because of long-range cavity
23 photon mediation, the internal states (pseudo-spins) are infinitely coordinated. The most famous example
24 is the Dicke model [6], which has been realized in CQED as well [7].

25   Another recent breakthrough in cold atoms stems from the realization of artificial (synthetic) gauge
26 potentials for neutral atoms, first in bosonic systems [8,9] and later in fermionic counterparts [10,11].
27 Laser fields are properly aligned and designed in such a way that trapped atoms may mimic charged
28 particles in a magnetic field with emergence of Lorentz-like force. The synthesis is achieved by inducing
29 two-photon Raman transition between two hyperfine ground states. Using a group of degenerate
30 (or quasi-degenerate) pseudo-spin eigenstates, non-abelian dynamics of cold atoms in light fields is
31 generated, which effectively leads to the spin-orbit coupling (SOC) for cold atoms, simulating the
32 electronic counterpart in condensed matter. Here, synthetic SOC refers to the coupling between atom's
33 pseudo-spins (i.e. hyperfine states) and COM motion, rather than the generic interaction between
34 electron's spin (or magnetic moment) and angular/linear momentum operator in quantum mechanics.
35 SOC is essential in understanding numerous underlying noval quantum phenomena and particle physics
36 [12], including *inter alia* topological insulators, Majorana and Weyl fermions, spin-Hall effects, etc
37 [13–17].

38   In this work, we first briefly review our previous proposal [18], and theoretically explore the
39 full quantum mechanical treatment beyond semi-classical mean field formalism, then investigate the
40 correspondences in quantum and semi-classical regions. We consider a single atom (or an ensemble of $\mathcal{N}$
41 non-interacting bosons) being confined by a single-mode unidirectional ring cavity, whose cavity mode
42 together with an additional coherent laser beam form a pair of Raman beams that flips atomic transition
43 between $|\uparrow\rangle$ and $|\downarrow\rangle$ while transferring recoil momentum of $\pm 2\hbar q_r \hat{z}$ from and/or to photon field. Hence,
44 the so-realized effective coupling between atom's external and internal degrees of freedom is generated
45 by the quantized light field, which is affected by atomic dynamics in return. We show that, at mean field
46 level, the cavity-assisted SOC dramatically modifies the atomic dispersion relation, in particular, with
47 emergence of loop structures under certain circumstances. We systematically characterize the atomic
48 dispersion relation of atomic state and photon number, both as a function of atom's quasi-momentum.
49 For given cavity parameters, we found with increasing Raman coupling strength Ω, dispersion curve
50 changes from double minima to gapped double minima, looped structure, and gapless single minimum
51 in sequence. Furthermore, we carry out the full quantum mechanical treatment by solving master
52 equations of density operators, and find good agreement by comparing averaged photon number with
53 mean field results in limiting parameter regions. The two distinctively different approaches give us an
54 unified understanding of the atom-light effective non-linearity and induced dynamical instability in this
55 system. how do we cite papers by David Feder, Hui Zhai,Su Yi, etc in this paragraph?

56   The article is organized as the following: After briefly reviewing key ideas of our previous work and
57 semi-classical mean field approach in Sec. 2, we develop the full quantum mechanical formalism to the
58 physical system of interest in Sec. 3 and discuss about the intimate correspondence between the two in
59 Sec. 4, and finally conclude in Sec. 5.

2. Model Setup and Semi-classical Mean Field Formalism

We follow the effective model Hamiltonian proposed in [18],

$$
\begin{aligned}
\mathcal{H}_{\text{eff}} &= \sum_{\sigma} \int d\mathbf{r} \left[\psi_{\sigma}^{\dagger}(\mathbf{r}) \left(\frac{\mathbf{k}^2 + 2\alpha q_r k_z}{2m} + \alpha\delta \right) \psi_{\sigma}(\mathbf{r}) \right] + \frac{\Omega}{2} \int d\mathbf{r} \left[\psi_{\uparrow}^{\dagger}(\mathbf{r})\psi_{\downarrow}(\mathbf{r})c + h.c. \right] \\
&+ i\varepsilon_p(c^{\dagger} - c) - \delta_c c^{\dagger}c - i\kappa c^{\dagger}c,
\end{aligned}
\tag{1}
$$

where $\psi_{\sigma}(\mathbf{r})$ ($\sigma = \uparrow, \downarrow$) is the atomic operator after gauge transformation in rotating frame at pump frequency ω_p. $\alpha = \pm 1$ for $\sigma = \uparrow, \downarrow$, respectively. q_r denotes recoil momentum, δ represents the two-photon Raman detuning, ε_p refers to pumping rate, and δ_c is the cavity-pump detuning. Ω denotes the atom-photon coupling strength, however, the Raman coupling term $\frac{\Omega}{2} \int d\mathbf{r} \left[\psi_{\uparrow}^{\dagger}(\mathbf{r})\psi_{\downarrow}(\mathbf{r})c + h.c. \right]$ describes the cavity-assisted two-photon Raman transition processes, where cavity photon operators c and $c^{\dagger}$ is explicitly taken into consideration. It is this coupling that renders the resulting SOC *dynamic*. Furthermore, in the semi-classical approach, we have treated the leakage of cavity photon phenomenologically by introducing a cavity decay rate κ.
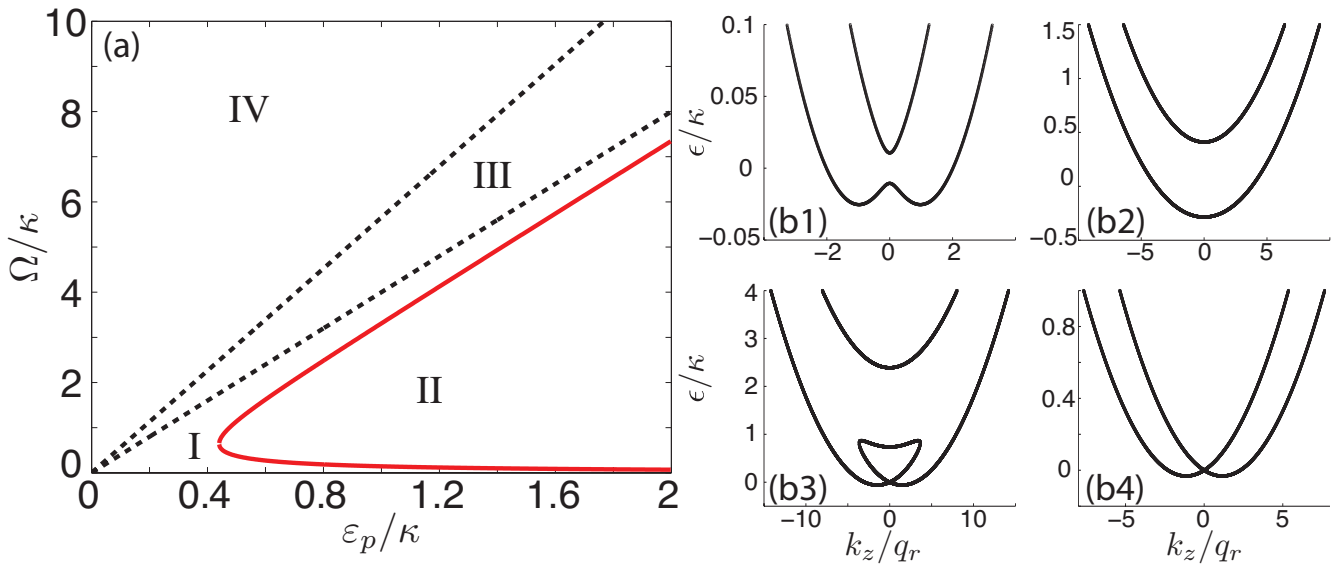

Figure 1. Single particle eigen-energy spectrum "phase diagram". For given paramter $\delta_c = \kappa$ and $\delta = 0$, the dispersion behavior is catagorized into four regions, represented from I to IV in (a). From (b1) to (b4), we fix $\varepsilon_p = \kappa$. In region I, the dispersion has double minima as shown in (b1) with $\Omega = 0.03\kappa$; region II is enclosed by the red solid curve in (a) and we show the typical point in (b2) ($\Omega = \kappa$) where only single minimum exisits in the lower helicity band; region III is enclosed by the black dashed lines in (a) and it is a region where loop structure emerge, as in (b3) with $\Omega = 5\kappa$; finally, in region IV we recover the double minimum dispersion although it's different from region I by closing the gap at $k_z = 0$, as in (b4) with $\Omega = 8\kappa$.

From the Hamiltonian (1), one can easily obtain the EOM in Heisenberg picture. To make progress, we adopt the mean-field approximation by replacing the operators by their respective expectation values: $c \to \langle c \rangle$, $\psi_{\sigma}(\mathbf{r}) \to \langle \psi_{\sigma}(\mathbf{r}) \rangle \equiv \varphi_{\sigma}(\mathbf{r})$. Assuming spatial homogeneity, we further take the plane-wave

wave-function for the atomic modes $\varphi_\sigma(\mathbf{r}) = e^{i\mathbf{k}\cdot\mathbf{r}}\varphi_\sigma$ with the normalization condition $|\varphi_\uparrow|^2 + |\varphi_\downarrow|^2 = \mathcal{N}$. The steady-state solution for the photon field is obtained by taking the time derivative of the photon field to be zero, which is exact by itself without making further approximations. After some algebra, we write the coupled nonlinear time-dependent equations for the two spin components as,

$$i\dot{\varphi}_\uparrow = \left(\frac{\mathbf{k}^2}{2m} + q_r k_z + \delta\right)\varphi_\uparrow + \frac{\Omega}{2}\frac{\varepsilon_p - i\frac{\Omega}{2}\mathcal{N}\varphi_\downarrow^*\varphi_\uparrow}{\kappa - i\delta_c}\varphi_\downarrow\,, \tag{2}$$

$$i\dot{\varphi}_\downarrow = \left(\frac{\mathbf{k}^2}{2m} - q_r k_z - \delta\right)\varphi_\downarrow + \frac{\Omega}{2}\frac{\varepsilon_p + i\frac{\Omega}{2}\mathcal{N}\varphi_\uparrow^*\varphi_\downarrow}{\kappa + i\delta_c}\varphi_\uparrow\,. \tag{3}$$

For a given atomic quasi-momentum $\mathbf{k}$, we define eigenstate and eigenenergy as the solution of the time-independent version of Eqs. (2) and (3), by replacing $i(\partial/\partial t)$ with $\epsilon(\mathbf{k})$. We consider $\mathcal{N} = 1$ and always take $k_x = k_y = 0$ hereafter. After some lengthy nonetheless straightforward algebra, we find that $\epsilon(\mathbf{k})$ obeys a quartic equation

$$4\epsilon^4 + B\epsilon^3 + C\epsilon^2 + D\epsilon + E = 0\,, \tag{4}$$

where detailed derivations are better elaborated in the Supplementary Material of [18].

We can gain some insights about the general structure of the dispersion relation $\epsilon(\mathbf{k})$, e.g. the degeneracy condition and the appearance and disappearance of the loop. Simple analysis shows that there should be a total of four regimes. (i) As denoted by region I in Fig. 1(a) and (b1), we show the dispersion curve exhibits a double minima structure. What is different from the degenercy condition given by the classical laser induced SOC Hamiltonian, is that for arbitrarily small Ω, there *always* are double minima in the dispersion. (ii) In region II of Fig. 1(a) and (b2), the dispersion curve has only single minimum. (iii) Region III corresponds to the region with loop structure and in Fig. 1(a) the two dashed black line are numerically obtained by examining the sign of second order derivative of the root with respect to k_z. When $\Omega_c^{(1)} \equiv 4\varepsilon_p \leq \Omega \leq 4\varepsilon_p\sqrt{1 + (\delta_c/\kappa)^2} \equiv \Omega_c^{(2)}$, at $k_z = 0$ there are total of four real roots allowed by the quartic equation — two degenerate roots at $\epsilon = 0$ and two additional roots with the same sign, see for instance Fig. 1(b3). (iv) Finally, when $\Omega > \Omega_c^{(2)}$ in region IV, only the two degenerate roots at $\epsilon(k_z = 0) = 0$ exist and we show the double minimum dispersion curve and gapless point at $k_z = 0$, see (b4) for instance.

The re-entrant behavior of the dispersion degeneracy can be understood by considering the effective Raman coupling strength $|\Omega_{\text{eff}}| \equiv \frac{\Omega}{2}\left|\frac{\varepsilon_p - i\frac{\Omega}{2}\varphi_\downarrow^*\varphi_\uparrow}{\kappa - i\delta_c}\right|$. To this end, in Fig. 2(a) we plot $|\Omega_{\text{eff}}|$ as a function of Ω for different k_z values (for illustration purposes we have chosen the lowest eigen-energy branch to compute the wave-functions $\varphi_\uparrow$ and $\varphi_\downarrow$). We note that $|\Omega_{\text{eff}}|$ does not monotonically increase with Ω, but rather to increase to a maximum and decrease back to zero at large Ω limit. This is once again due to the dynamic feedback of photon field onto atom center degrees of freedom. At small limit of Ω, atom-photon coupling is weak and atomic states with different k_z behave universally the same so that the atom photon field is effectively decoupled, which can be evidenced from the same linear slope $d|\Omega_{\text{eff}}|/d\Omega$ in the small Ω limit. On the other hand, when Ω becomes exceedingly large, such that photon is blocked away from entering the cavity (known as photon blockade), effective coupling between atom and photon is rather small and atomic bare spin state dominates over dressed state basis. In between these two limits, the re-entrant behavior of degenerate and non-degenerate dispersion is manifested in terms of $|\Omega_{\text{eff}}|$'s non-monotonousness as a function of Ω.

104   We remark that the introduction of cavity photon feedback dramatically alters the dispersion relation,
105 where one we could obtain from current proposals concerning classical laser induced SOC setups. As a
106 matter of fact, due to cavity mediation, the emergent loop structure is a distinctive nonlinear feature of the
107 system. Furthermore, upon studying the linearized perturbative expansion on top of fixed point solution
108 to Eq. 2 and Eq. 3, we have found intriguing dynamical stability properties, where there *always* exist
109 both dynamically stable and unstable branches regardless whether there is loop or not [18]. Nonetheless,
110 if we consider the large limit of pumping rate ε_p, we will again be able to recover classical laser induced
111 SOC limit. In this scenario, cavity photon field becomes the coherent state and atomic dressed state
112 appears as bare spin state such that $|\Omega_{\text{eff}}| \to \frac{\Omega}{2} \frac{\varepsilon_p}{\sqrt{\kappa^2+\delta_c^2}}$ in this limit. Then one can recover the degeneracy
113 condition for classical laser induced SOC Hamiltonian. When $\Omega < 4E_r \frac{\sqrt{\kappa^2+\delta_c^2}}{\varepsilon_p}$ dispersion curve has
114 degenerate double minimum; When $\Omega > 4E_r \frac{\sqrt{\kappa^2+\delta_c^2}}{\varepsilon_p}$ we only have a single minimum in the dispersion
115 curve. As we show in Fig. 2(b), the cavity-assisted SOC determined boundary curve asymptotically
116 approaches the blue dashed line which is given by the classical correspondence of large pumping rate
117 limit of $4E_r \frac{\sqrt{\kappa^2+\delta_c^2}}{\varepsilon_p}$. Note, in large ε_p limit, dynamical instability decay rate γ is also strongly suppressed
118 to a small value, such that the system fully recovers the synthetic SOC Hamiltonian.
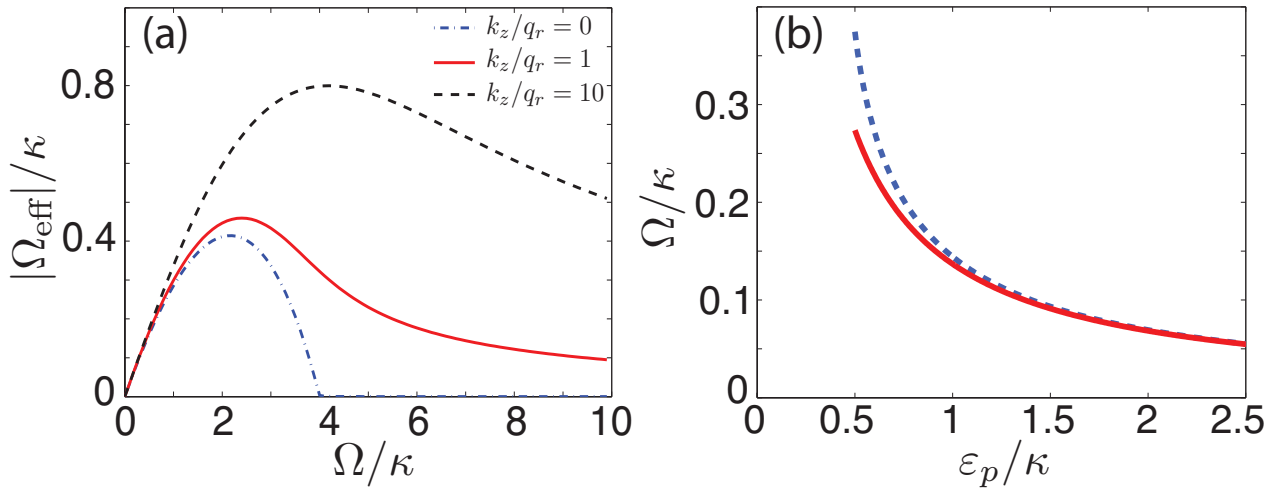

Figure 2. (a) Effective Raman coupling $|\Omega_{\text{eff}}|$ is plotted as a function of atom-photon coupling strength Ω for different k_z values, $0, q_r, 10q_r$ for blue dash-dot, red solid and black dashed lines. We observe that $|\Omega_{\text{eff}}|$ does not monotonically increases with Ω but rather peaks at an intermediate value, then approaches zero in the large Ω limit. Figure (b) shows a comparison between critical boundary of region I and II (red curve) and large pumping rate limit of $|\Omega_{\text{eff}}|$ (blue dashed line). At large ε_p limit, the two results match asymptotically well.

119   As we will also emphasize in Sec. 4, the synthesis of cavity confinement and Raman coupling is not
120 a trivial combination, but rather gives rise tonontrivial physics that deserves more scrutiny. In order to
121 better address the intricate coupling between atom and photon, we dedicate the Sec. 3 and Sec. 4 to
122 explore more on the quantum nature of this system.

123 **3. Master Equation Approach: Full Quantum Mechanical Treatment**

124 Semi-classical mean field approach gives an intuitive picture of understanding the atom-light
125 interaction, as we have shown above. However, it ignores quantum fluctuations of both operators c and
126 $\psi_\sigma(\mathbf{r})$. A more stringent approach is given by solving quantum master equation. The quantum master
127 equations, in a nutshell, are differential equations for the density operators, including contributions
128 from off-diagonal elements which represents quantum coherence characteristically. Master equation
129 is generally considered to be more general than the Schrödinger equation, since it uses the density
130 operator instead of a specific state vector and can therefore give statistical as well as quantum mechanical
131 information.

Instead of treating the leakage of cavity photon phenomenologically in Eq. (1), we model the
dissipation process by Liouvillean terms $\mathcal{L}$ appearing in the Lindblad master equation for the atom-field
density operator, i.e.,

$$\dot{\rho} = \frac{1}{i\hbar}[H_{\text{eff}}, \rho] + \mathcal{L}\rho. \tag{5}$$

where H_{eff} is the same as $\mathcal{H}_{\text{eff}}$ in Eq. (1) by dropping the last term, i.e. $-i\kappa c^\dagger c$. Cavity loss is
accommodated by the standard form of Lindblad superoperator [19,20],

$$\mathcal{L}\rho = \kappa(2c\rho c^\dagger - c^\dagger c\rho - \rho c^\dagger c). \tag{6}$$

132 Again, due to spatial homogeneity, we decouple momentum eigenstates by taking the plane-wave ansatz
133 for the atomic modes as $\varphi_\sigma(\mathbf{r}) = e^{i\mathbf{k}\cdot\mathbf{r}}\varphi_\sigma$. Thereon, we are granted to work under the Hilbert subspace
134 of a given momentum value $\mathbf{k}$. Here we explicitly write the commutator as,

$$
\begin{aligned}
[H_{\text{eff}}(\mathbf{k}), \rho] &= \left(\frac{\mathbf{k}^2}{2m} + \frac{q_r k_z}{m} + \delta\right)\left(\varphi_\uparrow^\dagger \psi_\uparrow \rho - \rho\varphi_\uparrow^\dagger \psi_\uparrow\right) + \left(\frac{\mathbf{k}^2}{2m} - \frac{q_r k_z}{m} - \delta\right)\left(\psi_\downarrow^\dagger \varphi_\downarrow \rho - \rho\varphi_\downarrow^\dagger \varphi_\downarrow\right) \\
&+ \mathcal{N}\frac{\Omega}{2}\left(\varphi_\uparrow^\dagger \varphi_\downarrow c\rho + c^\dagger \varphi_\downarrow^\dagger \varphi_\uparrow \rho - \rho\varphi_\uparrow^\dagger \varphi_\downarrow c - \rho c^\dagger \varphi_\downarrow^\dagger \varphi_\uparrow\right) \\
&+ i\varepsilon_p\left(c^\dagger \rho - c\rho - \rho c^\dagger + \rho c\right) - \delta_c\left(c^\dagger c\rho - \rho c^\dagger c\right).
\end{aligned}
\tag{7}
$$

135 To solve the operator equation, Eq. 5, we choose our basis state as direct product state $|n; \sigma\rangle$, where
136 non-negative integer n denotes photon number and atomic pseudo-spin state is represented by $\sigma = \uparrow, \downarrow$.
137 Our goal is to calculate the entire matrix elements of density operator under this set of basis states,
138 denoted by $\langle m; \sigma|\rho|n; \sigma'\rangle \equiv \rho_{mn}^{\sigma\sigma'}$. Without loss of generality, we have taken atom number $\mathcal{N} = 1$ to
139 simplify discussions. We found the governing EOM can be written as,

$$
\begin{aligned}
\frac{d}{dt}\rho_{mn}^{\sigma\sigma'} &= -i\left(\frac{\mathbf{k}^2}{2m} + \frac{q_r k_z}{m} + \delta\right)(\delta_{\sigma\uparrow} - \delta_{\sigma'\uparrow})\rho_{mn}^{\sigma\sigma'} - i\left(\frac{\mathbf{k}^2}{2m} - \frac{q_r k_z}{m} - \delta\right)(\delta_{\sigma\downarrow} - \delta_{\sigma'\downarrow})\rho_{mn}^{\sigma\sigma'} \\
&+ \frac{\Omega}{2i}(\delta_{\sigma\uparrow}\sqrt{m+1}\rho_{m+1n}^{\bar{\sigma}\sigma'} + \delta_{\sigma\downarrow}\sqrt{m}\rho_{m-1n}^{\bar{\sigma}\sigma'} - \delta_{\sigma'\uparrow}\sqrt{n+1}\rho_{mn+1}^{\sigma\bar{\sigma}'} - \delta_{\sigma'\downarrow}\sqrt{n}\rho_{mn-1}^{\sigma\bar{\sigma}'}) \\
&+ \varepsilon_p\left(\sqrt{m}\rho_{m-1n}^{\sigma\sigma'} - \sqrt{m+1}\rho_{m+1n}^{\sigma\sigma'} + \sqrt{n}\rho_{mn-1}^{\sigma\sigma'} - \sqrt{n+1}\rho_{mn+1}^{\sigma\sigma'}\right) \\
&+ i\delta_c(m-n)\rho_{mn}^{\sigma\sigma'} + \kappa\left(2\sqrt{m+1}\sqrt{n+1}\rho_{m+1n+1}^{\sigma\sigma'} - (m+n)\rho_{mn}^{\sigma\sigma'}\right),
\end{aligned}
\tag{8}
$$

140 where $\bar{\sigma}$ represents the flip-spin value, i.e. $\bar{\uparrow} = \downarrow$ and $\bar{\downarrow} = \uparrow$.

141 With Eq. 8, we can study dynamical evolution of density operator ρ for a given initial state. For
142 instance, we can initiate the system with a pure state $|0; \uparrow\rangle$, construct density operator $\rho = |0; \uparrow\rangle\langle 0; \uparrow|$,

143 and let it evolve according to Eq. 8 until all components reach their respective steady state. Although at

144 $t = 0$ we have $\text{Tr}[\rho^2] = 1$, at later times, we will always have $\text{Tr}[\rho^2] < 1$ for nonzero κ, because cavity

145 decay term renders the system into mixed states.

146 Assuming the fate of time evolution gives the steady state solution, we can also solve the set of

147 equations after equating the RHS of Eq. 8 to zero. Numerically, this is achieved by introducing a large

148 truncation value N for maximum number of cavity photon under consideration, such that the problem

149 reduces to simple linear algebra manipulations. In the following, we mainly focus on the steady-state

150 solution of density operator and ignore the transient dynamics.

151 In order to further quantitatively characterize atom-photon interaction in this open system, we invoke

152 the entanglement measure for mixed-state, the so-called negativity [21], defined as $\mathcal{N}(\rho) = \frac{||\rho^{T_A}||_1 - 1}{2}$,

153 where $||\rho^{T_A}||_1$ denotes the trace norm of partial transpose of density operator with respect to atom party

154 (the same is true for photon party). Density matrix ρ itself gives all positive definite eigenvalues and

155 thus the trace norm $||\rho||_1 = \text{Tr}[\sqrt{\rho^\dagger \rho}] = \text{Tr}[\rho] = 1$. Although the partial transpose ρ^{T_A} still satisfies

156 $\text{Tr}[\rho^{T_A}] = 1$, it does not necessarily guarantee positive definiteness in eigenvalues. The trace norm is

157 written generally as $||\rho^{T_A}||_1 = 1 + 2\sum_i |\mu_i|$ where we have denoted negative eigenvalues as $\mu_i < 0$.

158 Thus, by definition, the negativity $\mathcal{N}(\rho)$ is equal to $\sum_i |\mu_i|$, which measures by how much ρ^{T_A} fails to be

159 positive definite. An immediate consequence for any separable (unentangled) state ρ_s is that $\mathcal{N}(\rho_s) = 0$,

160 while for unseparable mixed state, $\mathcal{N}(\rho)$ is believed to be a good entanglement measure.

4. Results and Discussions

162 With above preparations, we are now in a position to discuss about the results given by the two

163 approaches, and address their relationship. As we have shown above and also in previous work [18], the

164 cavity feedback dramatically modifies single particle dispersion relation. For instance, in intermediate

165 region of atom-photon coupling strength of Ω, a loop structure emerge from the center tip of the

166 eigenenergy spectrum. Additionally, in this effective nonlinear system, although atom-photon coupling

167 is linear, dispersion spectrum possesses intriguing stability/instability properties. What we have shown

168 in [18] also indicates that only part of the dispersion is stable for a given quasi-momentum state **k**.

169 The instability analysis prescribes a recipe to map out regions whether fluctuations around fixed point

170 solution would grow exponentially or not. Tout de suite, we apply the formalism developed in Sec. 2

171 and Sec. 3 to calculate photon number expectation value inside the cavity.

172 As we show in Fig. 3(a)-(c), we plot semi-classical mean field photon number $|\langle c \rangle|^2$ and quantum

173 mechanical master equation result $\text{Tr}[\rho n]$, against atom's dimensionless quasi-momentum k_z/q_r. From

174 semi-classical mean field result, with increasing magnitude of Ω, we sweep over regions with only two

175 real roots, four real roots and only one double root (at $\epsilon = 0$) to the mean field solution of the quartic

176 equation. We can further perform dynamical analysis [18] to pinpoint stable (black dots) and unstable

177 branches of the semi-classical solution. For unstable states, we use colorbar to denote the renormalized

178 decay rate γ/Ω where γ refers to the largest real eigenvalue of perturbed dynamical equation [18]. For

179 comparison, with the same parameter set, we start from quantum master equation Eq. 8, and obtain steady

180 state solution of density operator, and trace over the product of density operator and photon number, i.e.

181 $\langle n \rangle = \text{Tr}[\rho n]$. Unlike semi-classical mean field theory, we can only have one unique solution of steady
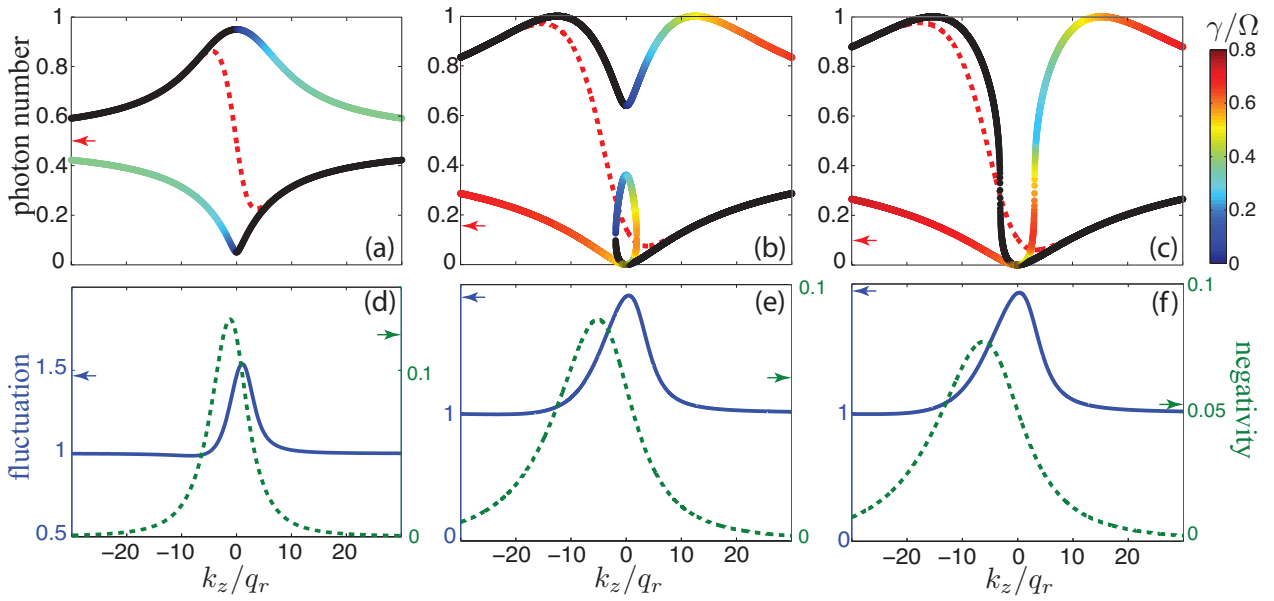
Figure 3. Photon number comparison between semi-classical mean field result and full quantum mechanical master equation solution. From (a) to (c), $\Omega = 3\kappa$, 5.6κ, 6κ and colorbar represents the renormalized decay rate γ/Ω of unstable states and red dashed lines are master equation solutions. Figures from (d) to (f) show the corresponding photon number fluctuation (blue solid curve) and negativity (green dashed line). Other parameters are $\varepsilon_p = \kappa$, $\delta_c = \kappa$, $\delta = 0$ and $\kappa = 1$ in the dimensionless unit. Although we have chosen $q_r = 0.22$ in our units (based on a realistic experimental parameter estimate) throughout all figures, we use arrows on vertical axis to denote results concerning $q_r = 0$ limit.

state density operator, thus only one branch of average photon number is found as a function of k_z, as represented by the red dashed line in Fig. 3(a)-(c).

We found, remarkably, that $\text{Tr}[\rho n]$ asymptotically approaches $|\langle c \rangle|^2$ value in dynamically stable branches at large $|k_z|$ limit. This agreement, first of all, further validates our previous dynamical stability analysis of semi-classical mean field result [18]. Due to momentum exchange of $\pm 2\hbar q_r \hat{z}$ in the Raman process, atomic states with small quasi-momentum $|k_z|$ are more coupled with photon field, in comparison to the states with large $|k_z|$. One would have naively thought cavity-assisted SOC should naturally provide more coupling between atom and photon field than the system with synthetic SOC, because atomic pseudo-spin state and COM are both coupled to cavity photon here. However, it is the SOC that renders this coupling *depends* on atomic quasi-momentum: (i) Momentum exchange plays a major role at small k_z where two SOC bands are avoided-crossing, and eigenstate is a strong hybridization between bare atomic pseudo-spin states. Thus atom and photon is strongly coupled in this region. (ii) While at large k_z limit, energy separation becomes so large that the two dressed states are more like two independent bare atomic pseudo-spin states $|\uparrow\rangle$ and $|\downarrow\rangle$. Atomic spin state, COM and photon field are all decoupled in this limit.

Second, the relationship between semi-classical mean field result and quantum master equation result can be understood from photon number fluctuation, which by definition is given by $\frac{\langle(\Delta n)^2\rangle}{\langle n \rangle} = \frac{\langle n^2 \rangle - \langle n \rangle^2}{\langle n \rangle}$. In Fig. 3(d)-(f), on the left y-axis, we plot the renormalized fluctuation magnitude as a function of k_z, shown as blue solid curve. We found it degrades to one in large $|k_z|$ limit, and this is the limit where photon state is best modeled by the coherent state (Poissonian statistics) and atom's back-action *onto* photon becomes negligibly small. For small $|k_z|$ values, the majority part of fluctuation is larger than one, which implies a super-Poissonian photon number distribution, where cavity photon behaves more thermal like, which is far away from coherent state. If we have a positive definite probability distribution for photon number, by the application of Cauchy-Schwarz inequality, the fluctuation value would always have to be greater or equal to one. However, there are regions where renormalized fluctuation is smaller than one, e.g. in Fig. 3(d) at small negative k_z value, $\frac{\langle(\Delta n)^2\rangle}{\langle n \rangle} \sim 0.95$, which implies sub-Poissonian photon number distribution as a signature of system being genuinely non-classical.

Third, the degree of entanglement for a mixed-state can be quantitatively characterized by the negativity $\mathcal{N}(\rho)$ [21], which we briefly mentioned in Sec. 3. In Fig. 3(d)-(f), on the right y-axis, we plot the negativity against k_z/q_r for different Ω values using green dashed lines. We can see that when photon field approaches its coherent state at large $|k_z|$, negativity becomes very close to zero which means the "atom + photon" system becomes separable. When photon fluctuation deviates from one, negativity shows up a pronounced peak in a qualitatively similar manner.

Above observations conclude our discussion on the relationship between semi-classical theory and quantum mechanical master equation approach in the proposed cavity-assisted SOC system. Alternatively, we can also comment on the relationship between cold atom cavity QED physics and the current work. Conventionally, J-C Model is used to describe interaction between a two level atomic state and photon field by ignoring the rest degrees of freedom. In lieu of mimicking J-C Model, we set q_r to zero in the Hamiltonian and repeat the steady state solution to Eq. 5. Under this setting, atom's kinetic energy only contribute to a dynamical phase that does not affect expectation value of observable, e.g. photon number, fluctuation, etc. Then we choose an arbitrary value of k_z or ignore $k_z^2/2m$ term

altogether, and compute $\text{Tr}[\rho n]$, $\frac{\langle(\Delta n)^2\rangle}{\langle n\rangle}$ and $\mathcal{N}(\rho)$ where we use arrows on the y-axis to denote their values in Fig. 3. As we can observe in Fig. 3 from (a) to (c), photon number in J-C Model limit is very different from the one by considering cavity-assisted SOC, *even* in large k_z asymptotic limit. We have $\text{Tr}[\rho n] \approx 0.49, 0.14, 0.11$ from (a) to (c), while we always have asymptotic value of $\frac{\varepsilon_p^2}{\kappa^2+\delta_c^2}$ *independent* of Ω value in our system, which is 0.5 in Fig. 3. However, we are able to recover J-C model by simultaneously setting both q_r and Ω to zero, where there is only generic atomic spin and photon coupling present. In Fig. 3 from (d) to (f), we have $\frac{\langle(\Delta n)^2\rangle}{\langle n\rangle} \approx 1.47, 1.91, 1.93$ and $\mathcal{N}(\rho) \approx 0.12, 0.06, 0.05$, respectively.

5. Conclusion and Outlook

In this work, we have studied spin-orbit coupled cold atoms inside a ring cavity system, employing both semi-classical mean field theory and full quantum mechanical master equation approach. By treating both light and atom on equal footing and seeking the self-consistent solution in both approaches, we have found cavity-assisted SOC dramatically modified atomic dispersion relation, intriguing dynamical instabilities, and atom's back-action onto light field also leads to non-trivial atom-photon coupling that are fundamentally different to the system with either synthetic SOC or J-C model type of interaction. We have also explored correspondence and discussed the relationship between the two approaches. We conclude that the synthesis of cavity QED and SOC is not a trivial combination and interesting new physics are emergent in this setting. The two distinctively different approaches give us an unified understanding of the atom-light effective non-linearity and induced dynamical instability in this system.

Although for simplicity reasons we have only considered one atom inside the cavity, the current mean field formalism and results can be easily generalized to $\mathcal{N}$ identical non-interacting bosons, where we would expect similar physics involving atom and light couplings. However, due to anti-symmetrization constraint, for $\mathcal{N}$ non-interacting fermions, it is less straightforward to bridge a connection. Furthermore, it would be interesting to consider atom-atom interactions for the many body case cite Feder's paper here? and study super-radiant Dicke phase transition cite Hui Zhai's paper and Xiong-Jun Liu's super-radiant paper here?, using the master equation approach.

Author Contributions

H.P. conceived the idea of the project, L.D. and C. Z. explored the theoretical and numerical aspects of the physics. All authors contributed to writing and revising the manuscript and participated in the discussions about this work.

Conflicts of Interest

The authors declare no conflict of interest.

References

1. E.T. Jaynes, F.W. Cummings (1963). Proc. IEEE 51 (1): 89âĂŞ109.
2. G. Rempe, H. Walther, and N. Klein (1987). Phys. Rev. Lett. 58 (4): 353âĂŞ356.
3. Brennecke, F., Donner, T., Ritter, S., Bourdel, T., Kohl, M., and Esslinger, T., *Nature* **2007**, *450* 268.
4. Colombe, Y., Steinmetz, T., Dubois, G., Linke, F., Hunger, D. and Reichel, J. *Nature* **2007**, *450* 272.
5. Slama, S., Bux, S., Krenz, G., Zimmermann, C. and Courteille, Ph. W. *Phys. Rev. Lett.* **2007**, *98* 053603.
6. Dicke, R. H. Coherence in spontaneous radiation processes. Phys. Rev. 93, 99âĂŞ110 (1954).
7. Kristian Baumann, Christine Guerlin, Ferdinand Brennecke Tilman Esslinger. Nature 464, 1301âĂŞ1306 (29 April 2010)
8. Y.-J. Lin, K. Jimenez-Garcia, and I. B. Spielman, *Nature* (London) **2011**, *471*, 83.
9. Y.-J. Lin, R. L. Compton, K. Jimenez-Garcia, W. D. Phillips, J. V. Porto, and I. B. Spielman, *Nat. Phys.* **2011**, *7*, 531.
10. P. Wang, Z.-Q. Yu, Z. Fu, J. Miao, L. Huang, S. Chai, H. Zhai, and J. Zhang, *Phys. Rev. Lett.* **2012**, *109*, 095301.
11. L. W. Cheuk, A. T. Sommer, Z. Hadzibabic, T. Yefsah, W. S. Bakr, and M. W. Zwierlein, *Phys. Rev. Lett.* **2012**, *109*, 095302.
12. V Galitski, IB Spielman, *Nature* **2013**, *494* 7435.
13. Hasan, M. Z., Kane, C. L. *Rev. Mod. Phys.* **2010**, *82* 3045âĂŞ3067.
14. Sau, J. D., Lutchyn, R. M., Tewari, S. and Sarma, Das, S. *Phys. Rev. Lett.* **2010**, *104* 040502.
15. Burkov, A. A. and Balents, L., *Phys. Rev. Lett.* **2011**, *107* 127205.
16. Sinova, J., Cilcer, D., Niu, Q., Sinitsyn, N., Jungwirth, T., and MacDonald, A., *Phys. Rev. Lett.* **2004**, *92* 126603.
17. Kato, Y. K., Myers, R. C., Gossard, A. C. and Awschalom, D. D., *Science* **2004**, *306* 1910âĂŞ1913.
18. Lin Dong, Lu Zhou, Biao Wu, B. Ramachandhran, and Han Pu, *Phys. Rev. A* **2014** *89*, 011602(R).
19. Kossakowski, A. Rep. Math. Phys. **1972**, *3* (4): 247.
20. Lindblad, G. *Commun. Math. Phys.* **1976**, *48* (2): 119.
21. Vidal, G., Werner, R. F., *Phys. Rev. A* **2002**, *65* 032314.